Zero-field muon-spin-relaxation depolarization rate of paramagnets near the Curie temperature

A. Yaouanc and P. Dalmas de Réotier
Centre d'Etudes Nucléaires, DRFMC/SPSMS/LIH, Boîte Postale No. 85X, F-38041 Grenoble-CEDEX, France

E. Frey*
Lyman Laboratory of Physics, Harvard University, Cambridge, Massachusetts 02138
(Received 3 August 1992)

The paramagnetic critical zero-field muon-spin-relaxation damping rate for cubic ferromagnets with dipolar interactions is computed by mode-coupling theory. We show that the temperature behavior of the damping rate is determined by the relative weight of the hyperfine interaction and the dipolar interaction between the muon magnetic moment and the lattice ion magnetic moments. A quantitative interpretation of the experimental data recorded on metallic Ni and Fe is given. Predictions are made for EuO and EuS.

I. INTRODUCTION

The critical dynamics of isotropic ferromagnets above the Curie temperature (T_C) has been studied by various experimental techniques, sampling different regions in wave-vector space.[1-3] At first sight the results of these different studies did not seem consistent. It is only recently that an overall satisfactory explanation of the experimental data has been reached.[4,5] It has been shown that the dipolar interaction between the lattice dipole magnetic moments, which has a negligible effect on the T_C value, has a strong influence on the paramagnetic critical dynamics for small wave-vector modes. This is a consequence of the dipolar interaction, which is present in all real ferromagnets, being of long range.

Up to now the experimental work has been mostly performed on isotropic ferromagnets using three types of experimental techniques: electron-spin-resonance (ESR) and magnetic relaxation,[1] hyperfine interaction (HI) methods,[2] and neutron scattering.[3] ESR measurements are restricted to nonmetallic compounds. Two HI techniques have been mostly used: perturbed angular correlation (PAC) and Mössbauer spectroscopy (MS). The results obtained by these two techniques have nicely shown that, while the amount of information deduced from them is more restricted than the one obtained from neutron-scattering experiments, they probe the region near the center of the Brillouin zone which is most important for the dynamics of ferromagnets near T_C. Present neutron-scattering techniques do not allow one to measure at sufficiently small wave vectors to directly study the effect of the dipolar interaction on the spin dynamics right at the critical temperature; its effect has been seen by neutron scattering only above T_C.[3]

The muon-spin-relaxation (μSR) method which is a HI technique,[6,7] has been used to probe the spin dynamics of Ni (Ref. 8) and Fe (Ref. 9) which have a cubic crystal structure and of Gd (Ref. 10) which crystallizes in an hexagonal lattice. As pointed out by Yushankhai,[11] an understanding of the μSR data requires one to take into account the classical dipolar interaction between the muon magnetic moment and the lattice ion magnetic moments. A recent study of the μSR depolarization rate at low temperature in a Heisenberg ferromagnet strengthens this point of view.[12,13] In the case of PAC and MS, the coupling interaction is mainly due to the HI which is, to a good approximation, isotropic and of short range. The difficulties to take into account the peculiarities of the dipolar interaction, i.e., its strong anisotropy and its long-range nature, may explain why μSR spectroscopy has not been used intensively to study the spin dynamics of ferromagnets. This is unfortunate because, opposite of other HI techniques, μSR measurements can be performed on any compound. A solid-state solution of the studied compound with atoms containing the nuclear probe does not have to be prepared.

Recently a theoretical prediction for the μSR damping rate in the paramagnetic critical regime of the Heisenberg ferromagnet EuO has been presented.[14] This analysis does not seem complete because it does not take into account the long-range nature of the dipolar interaction between the muon magnetic moment and the lattice magnetic moments. Furthermore, the dipolar interaction between these latter moments is neglected, which is known to have a major effect on the spin dynamics close to T_C and for a long wavelength.

The purpose of this report is to present a theoretical study of those effects on the zero-field μSR damping rate. Especially, we investigate the consequences of the symmetry and long-range nature of the dipolar interaction between the muon magnetic moment and the lattice ion magnetic moments for a paramagnet near T_C on the zero-field μSR damping rate. We suppose that the magnet can be described by an isotropic Heisenberg Hamiltonian. In addition, the dipolar interaction between the ions magnetic moments is included. For simplicity, we will suppose that the magnetic ions sit on a Bravais lattice.

The organization of this paper is as follows. In Sec. II, we express the zero-field μSR depolarization rate of a

paramagnet in terms of spin correlation functions. In Sec. III, we discuss the behavior in the wave-vector representation of the coupling between the muon magnetic moment and the lattice ion magnetic moments for wave vectors near the center of the Brillouin zone. In Sec. IV, we review the properties of the spin correlation functions in the paramagnetic critical regime of a cubic Heisenberg ferromagnet with the ion-ion dipolar interaction taken into account. In this section we summarize the quantitative predictions made by the mode-coupling theory. In Sec. V, we use the information previously gathered to compute the zero-field μSR damping rate of some isotropic magnets. A comparison between theory and experiment is performed when possible. The last section is devoted to a summary of our findings and to the conclusion. Mathematical details of the derivation of two formulas are given in two appendices.

II. ZERO-FIELD μSR DEPOLARIZATION RATE AND SPIN CORRELATION FUNCTIONS

In this section we show that the zero-field μSR depolarization function for a paramagnet depends on spin correlation functions of the localized spins and on a tensor which takes into account the coupling between the muon spin and the localized spins of the magnet. Thus, we explicitly assume that the depolarization induced by the dynamics of the electron spin at the muon site is negligible. This hypothesis may not always be valid.

We take the z axis parallel to the incoming muon beam polarization. We use an orthonormal reference frame. A zero-field measurement consists of measuring the depolarization function $P_z(t)$.[6,7] It can be shown that[15]

$$P_z(t)=\tfrac{1}{2}\mathrm{Tr}[\rho_m \sigma_z \sigma_z(t)] , \tag{2.1}$$

where ρ_m is the density operator of the magnet and σ_z the projection of the Pauli operator of the muon spin on the z axis. $\mathrm{Tr}[A]$ stands for the trace of A over the muon and magnet quantum states.

Usually $\sigma_z(t)$ can only be computed approximately. As the critical magnetic fluctuations are sufficiently rapid, the depolarization they induce can be treated in the motional narrowing limit. Thus, as in nuclear magnetic resonance (NMR), it is justified to compute $\sigma_z(t)$ by a second-order iteration. This computation gives[15,16]

$$P_z(t)=\exp[-\psi_z(t)] , \tag{2.2}$$

with

$$\psi_z(t)=\gamma_\mu^2 \int_0^t d\tau (t-\tau)[\Phi_{xx}(\tau)+\Phi_{yy}(\tau)] . \tag{2.3}$$

γ_μ is the muon gyromagnetic ratio; $\gamma_\mu=851.6$ Mrad $\mathrm{s}^{-1}\,\mathrm{T}^{-1}$. Here

$$\Phi_{\alpha\alpha}(\tau)=\tfrac{1}{2}[\langle \delta B_\alpha(\tau)\delta B_\alpha\rangle+\langle \delta B_\alpha\, \delta B_\alpha(\tau)\rangle] \tag{2.4}$$

is the symmetrized correlation function of the α component ($\alpha\in\{x,y,z\}$) of the fluctuating part of the local magnetic field at the muon site. $\langle A\rangle$ stands for the thermal average of A. The time evolution of the fluctuations is governed by the Heisenberg equation

$$\delta B_\alpha(\tau)=\exp(i\mathcal{H}_m\tau/\hbar)\delta B_\alpha \exp(-i\mathcal{H}_m\tau/\hbar) , \tag{2.5}$$

where $\mathcal{H}_m$ is the Hamiltonian that describes the magnetic properties of the magnet. The expression of $P_z(t)$ can usually be simplified because the characteristic time of the fluctuations is $\tau\approx 10^{-12}$ s whereas the experimental time window is $10^{-8}\lesssim t\lesssim 10^{-5}$ s. Therefore, we can neglect τ in the $(t-\tau)$ factor and extend the integral to infinity. Taking the fact that $\Phi_{\alpha\alpha}(\tau)=\Phi_{\alpha\alpha}(-\tau)$, we have, to a good approximation, $\psi_z(t)=\lambda_z t$ with

$$\lambda_z=\frac{\gamma_\mu^2}{2}\int_{-\infty}^{\infty} d\tau[\Phi_{xx}(\tau)+\Phi_{yy}(\tau)] . \tag{2.6}$$

Therefore, the depolarization function is an exponential function with the damping rate λ_z. If we identify λ_z with $1/T_1$, where T_1 is the muon-spin-lattice-relaxation time, the above μSR expression is equivalent to the NMR formula given by Moriya.[17]

We now introduce the time-Fourier transform of a function $f(\tau)$:

$$f(\omega)=\frac{1}{2\pi}\int_{-\infty}^{\infty} d\tau \exp(-i\omega\tau) f(\tau) . \tag{2.7}$$

Then λ_z can be written in terms of time-Fourier transforms at $\omega=0$

$$\lambda_z=\pi\gamma_\mu^2[\Phi_{xx}(\omega=0)+\Phi_{yy}(\omega=0)] . \tag{2.8}$$

From now on, we will deal with correlation and spectral weight functions in the frequency domain taken at $\omega=0$. For simplicity we will write $\bar{A}=A(\omega=0)$.

We now consider the magnetic interactions in the magnet. The muon spin couples to the localized spins through the classical dipolar interaction and the conduction electron spins via the Fermi contact interaction. This latter interaction leads to an effective coupling between the muon spin and the localized spins. As mentioned at the beginning of this section, we suppose that the dynamic effect (Korringa-type relaxation) of the electron spin on the muon spin is negligible. These two types of interactions produce a magnetic field at the muon site. The α component of its fluctuating part is given by

$$\delta B_\alpha=\frac{\mu_0}{4\pi}\frac{g_L\mu_B}{v}\sum_i \sum_{\beta=x,y,z} G_{\mathbf{r}_i}^{\alpha\beta}\delta J_{i,\beta} . \tag{2.9}$$

The index i runs over the lattice sites. The tensor $G_{\mathbf{r}_i}$ has the following components:

$$G_{\mathbf{r}_i}^{\alpha\beta}=D_{\mathbf{r}_i}^{\alpha\beta}+H_{\mathbf{r}_i}\delta^{\alpha\beta} , \tag{2.10}$$

with

$$D_{\mathbf{r}_i}^{\alpha\beta}=v\left[\frac{3r_{i,\alpha}r_{i,\beta}}{r_i^5}-\frac{\delta^{\alpha\beta}}{r_i^3}\right] =v\left[\frac{\partial^2}{\partial r_\alpha \partial r_\beta}\frac{1}{|\mathbf{r}|}\right]_{\mathbf{r}=\mathbf{r}_i} . \tag{2.11}$$

For simplicity, we suppose that the magnetic ions sit on a Bravais lattice (there is therefore only one type of mag-

netic ions) and that the Fermi contact interaction leads to an isotropic coupling between the muon spin and the nearest-neighbor localized spins to the muon site. Therefore, $H_{\mathbf{r}_i}$ is either equal to H if i refers to one of the nearest-neighbor atoms or zero otherwise. v is the volume of the primitive cell of the Bravais lattice; g_L the Landé factor of spin $\mathbf{J}_i$, which is at the distance vector $\mathbf{r}_i$ from the muon. μ_B is the Bohr magneton, μ_0 the permeability of free space, $r_{i,\alpha}$ the α component of $\mathbf{r}_i$, $\alpha,\beta=x,y,z$, and $|\mathbf{r}|=(x^2+y^2+z^2)^{1/2}$. With this formula for $\delta\mathbf{B}$, it is now possible to give an expression of $\tilde{\Phi}_{\alpha\alpha}$ in terms of symmetrized correlation functions of the spins, $\tilde{\Lambda}_{ij}^{\beta\gamma}$. We obtain

$$\tilde{\Phi}_{\alpha\alpha}=\left[\frac{\mu_0}{4\pi}\right]^2\frac{(g_L\mu_B)^2}{v^2}\sum_{i,j}\sum_{\beta,\gamma}G_{\mathbf{r}_i}^{\alpha\beta}G_{\mathbf{r}_j}^{\alpha\gamma}\tilde{\Lambda}_{ij}^{\beta\gamma}\ , \tag{2.12}$$

with

$$\tilde{\Lambda}_{ij}^{\beta\gamma}=\tfrac{1}{2}[\langle\delta J_{i,\beta}(\omega=0)\delta J_{j,\gamma}\rangle+\langle\delta J_{j,\gamma}\,\delta J_{i,\beta}(\omega=0)\rangle]\ . \tag{2.13}$$

In general, a calculation of a spin correlation function is performed in the $(\mathbf{q},\omega)$ space, i.e., in the first Brillouin zone and in the frequency domain. Therefore, we need to introduce the spatial-Fourier transform of the correlation functions. We notice that the muon localizes in an interstitial site. Hence, as this site does not belong to the lattice, some care has to be exercised. In Fig. 1, we define the two types of sites and vectors involved. The origin of the reference frame is taken at the lattice 0 site. Two types of vectors are present in the problem: the lattice vectors as, for example, $\mathbf{i}$, and the vectors linking the muon site to the lattice sites, $\mathbf{r}_i$, for instance. With these definitions we set

$$\delta J_{i,\alpha}=\frac{1}{N}\sum_{\mathbf{q}}\exp(i\mathbf{q}\cdot\mathbf{i})\delta J_{\mathbf{q},\alpha}\ . \tag{2.14}$$

The $\mathbf{q}$ sum extends over N vectors of the first Brillouin zone. Taking into account the facts that $\tilde{\Lambda}_{ij}^{\beta\gamma}$ depends only on $(\mathbf{i}-\mathbf{j})$ and the $\mathbf{i}-\mathbf{j}=\mathbf{r}_i-\mathbf{r}_j$ (see Fig. 1), we obtain using Eq. (2.14)

$$\tilde{\Lambda}_{ij}^{\beta\gamma}=\frac{1}{N^2}\sum_{\mathbf{q}}\exp[i\mathbf{q}\cdot(\mathbf{r}_i-\mathbf{r}_j)]\tilde{\Lambda}_{\mathbf{q}}^{\beta\gamma}\ , \tag{2.15}$$

with

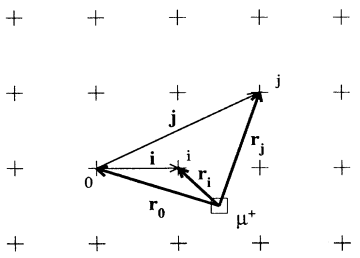

FIG. 1. Definition of vectors relative to the crystallographic (+) and muon (□) sites.

$$\tilde{\Lambda}_{\mathbf{q}}^{\beta\gamma}=\tfrac{1}{2}[\langle\delta J_{\mathbf{q},\beta}(\omega=0)\delta J_{-\mathbf{q},\gamma}\rangle+\langle\delta J_{-\mathbf{q},\gamma}\,\delta J_{\mathbf{q},\beta}(\omega=0)\rangle]\ . \tag{2.16}$$

In zero magnetic field, time-reversal symmetry tells us that $\tilde{\Lambda}_{\mathbf{q}}^{\beta\gamma}=\tilde{\Lambda}_{\mathbf{q}}^{\gamma\beta}$. Using the previous equations, we are now in a position to express $\tilde{\Phi}_{\alpha\alpha}$ with the $\mathbf{q}$ variable. We find

$$\tilde{\Phi}_{\alpha\alpha}=\left[\frac{\mu_0}{4\pi}\right]^2\frac{(g_L\mu_B)^2}{V^2}\sum_{\mathbf{q}}\sum_{\beta,\gamma}G_{\mathbf{q}}^{\alpha\beta}G_{-\mathbf{q}}^{\alpha\gamma}\tilde{\Lambda}_{\mathbf{q}}^{\beta\gamma}\ , \tag{2.17}$$

where we have defined

$$G_{\mathbf{q}}^{\alpha\beta}=\sum_i G_{\mathbf{r}_i}^{\alpha\beta}\exp(i\mathbf{q}\cdot\mathbf{r}_i)\ . \tag{2.18}$$

V is the volume of the sample. Introducing Eq. (2.17) in Eq. (2.8), we derive

$$\lambda_z=\frac{\pi\mathcal{D}}{V^2}\sum_{\mathbf{q}}\sum_{\beta,\gamma}(G_{\mathbf{q}}^{x\beta}G_{-\mathbf{q}}^{x\gamma}+G_{\mathbf{q}}^{y\beta}G_{-\mathbf{q}}^{y\gamma})\tilde{\Lambda}_{\mathbf{q}}^{\beta\gamma}\ , \tag{2.19}$$

where we have defined $\mathcal{D}=(\mu_0/4\pi)^2\gamma_\mu^2(g_L\mu_B)^2$. This equation shows that the measured μSR damping rate depends on the coupling between the muon spin and the spins of the magnet through the tensor $G_{\mathbf{q}}$ and on spin correlation functions of the magnet itself, $\tilde{\Lambda}_{\mathbf{q}}^{\alpha\beta}$. As it is well known, such a formula is found for the other HI techniques.[2] The difference between μSR and these other techniques resides in the fact that, in the present case, $G_{\mathbf{q}}$ has peculiar properties at small-$\mathbf{q}$ value. This latter point is important for a ferromagnet near T_C.

It is practical, for the evaluation of the sum over $\mathbf{q}$ in Eq. (2.19), to consider $\mathbf{q}$ as a continuous variable and therefore to replace the sum by an integral. Then Eq. (2.19) becomes

$$\begin{aligned}\lambda_z&=\frac{\pi\mathcal{D}}{V}\int\frac{d^3q}{(2\pi)^3}\sum_{\beta,\gamma}[G^{x\beta}(\mathbf{q})G^{x\gamma}(-\mathbf{q})\\&\qquad+G^{y\beta}(\mathbf{q})G^{y\gamma}(-\mathbf{q})]\tilde{\Lambda}^{\beta\gamma}(\mathbf{q})\\&=\frac{\pi\mathcal{D}}{V}\int\frac{d^3q}{(2\pi)^3}\{[G(\mathbf{q})\tilde{\Lambda}(\mathbf{q})G(-\mathbf{q})]^{xx}\\&\qquad+[G(\mathbf{q})\tilde{\Lambda}(\mathbf{q})G(-\mathbf{q})]^{yy}\}\ .\end{aligned} \tag{2.20}$$

The integrals extend over the first Brillouin zone. The second line of Eq. (2.20) expresses λ_z in terms of the diagonal elements of the product of tensors. To arrive to this compact formula we have used the following symmetry property: $G^{\alpha\beta}(\mathbf{q})=G^{\beta\alpha}(\mathbf{q})$. From now on, we will consider the $G(\mathbf{q})$ and $\tilde{\Lambda}(\mathbf{q})$ tensors as continuous functions of $\mathbf{q}$.

At first sight Eqs. (2.19) and (2.20) may look wrong because λ_z is inversely proportional to the sample volume V. But we shall see at Eq. (4.8) that a correlation function is proportional to N. Therefore, λ_z is proportional to $N/V=1/v$. In the next section we present a detailed study of the tensor $G(\mathbf{q})$ for selected cases.

III. MUON-LATTICE INTERACTION AT SMALL-q VECTOR

The tensor $G(\mathbf{q})$ is the sum of the dipolar and hyperfine tensors. We first consider the dipolar tensor $D(\mathbf{q})$.

The computation of the dipolar tensor in the $\mathbf{q}$ representation, which is defined by Eqs. (2.10), (2.11), and (2.18), is given in Appendix A. The $\mathbf{q}$ summation is made following Ewald's method.[18,19] $D^{\alpha\beta}(\mathbf{q})$ is the sum of four terms:

$$D^{\alpha\beta}(\mathbf{q})=-4\pi\frac{q_\alpha q_\beta}{q^2}+4\pi\frac{q_\alpha q_\beta}{q^2}\left[1-\exp\left[\frac{-q^2}{4\rho^2}\right]\right]-\frac{\pi}{\rho^2}\sum_{\mathbf{K}\neq 0}(K_\alpha+q_\alpha)(K_\beta+q_\beta)\varphi_0\left[\frac{(\mathbf{q}+\mathbf{K})^2}{4\rho^2}\right]\exp(-i\mathbf{K}\cdot\mathbf{r}_0)$$
$$+\frac{2v\rho^3}{\sqrt{\pi}}\sum_i\left[2\rho^2 r_{i,\alpha}r_{i,\beta}\varphi_{3/2}(\rho^2 r_i^2)-\delta^{\alpha\beta}\varphi_{1/2}(\rho^2 r_i^2)\right]\exp(i\mathbf{q}\cdot\mathbf{r}_i)\ . \tag{3.1}$$

The $\varphi_m(x)$ functions are defined by Eq. (A6) of Appendix A. Expression (3.1) gives the same result for all values of the Ewald parameter ρ, but for numerical applications a value of ρ is chosen which ensures that both series converge rapidly. The first term of $D^{\alpha\beta}(\mathbf{q})$ is only piecewise continuous at $\mathbf{q}=\mathbf{0}$. Its average value in the neighborhood of $\mathbf{q}=\mathbf{0}$ is $-(4\pi/3)\delta^{\alpha\beta}$. Using Eq. (3.1) it is possible to compute $D^{\alpha\beta}(\mathbf{q})$ for any value of $\mathbf{q}$. It is convenient to write

$$D^{\alpha\beta}(\mathbf{q})=-4\pi\left[\frac{q_\alpha q_\beta}{q^2}-C^{\alpha\beta}(\mathbf{q})\right]\ , \tag{3.2}$$

where $C^{\alpha\beta}(\mathbf{q})$ is a symmetric tensor whose elements are continuous functions of $\mathbf{q}$.

In a ferromagnet near T_C, nuclear methods such as μSR spectroscopy probe the behavior of correlation functions near the center of the Brillouin zone.[2] Hence, as it will be clear from the work presented in the next section, there is a special interest to look at $D^{\alpha\beta}(\mathbf{q})$ for small-$\mathbf{q}$ values. In this paper we restrict our study to the lowest order in $\mathbf{q}$. This should be sufficient because we are only interested in the behavior of the μSR damping rate near T_C.

The lowest-order approximation in $\mathbf{q}$ of $D^{\alpha\beta}(\mathbf{q})$ is given by

$$D^{\alpha\beta}(\mathbf{q}\to\mathbf{0})=-4\pi\left[\frac{q_\alpha q_\beta}{q^2}-C^{\alpha\beta}(\mathbf{q}=\mathbf{0})\right]\ . \tag{3.3}$$

Because the trace of $D(\mathbf{q}=\mathbf{0})$ is equal to zero,[21] the following relation holds:

$$\sum_\alpha C^{\alpha\alpha}(\mathbf{q}=\mathbf{0})=1\ . \tag{3.4}$$

Because the $C(\mathbf{q}=\mathbf{0})$ and $D(\mathbf{q}=\mathbf{0})$ tensors are related by Eq. (3.3), we can use symmetry properties of the latter tensor to derive information on the former tensor. $D(\mathbf{q}=\mathbf{0})$ has been studied in detail for a muon in a tetrahedral or an octahedral interstitial site of a face-centered- or a body-centered-cubic crystal,[21] fcc and bcc, respectively. In this paper we only consider these cases.

In the case of a fcc crystal we derive $C^{\alpha\beta}(\mathbf{q}=\mathbf{0})=(\frac{1}{3})\delta^{\alpha\beta}$ for a muon either in a tetrahedral or octahedral site.

The situation is not so simple for a bcc crystal. We suppose here that the z axis lies along one of the three $\langle 100\rangle$ axes. We have

$$D^{xx}(\mathbf{q}=\mathbf{0})=D^{yy}(\mathbf{q}=\mathbf{0})=-D^{zz}(\mathbf{q}=\mathbf{0})/2\ . \tag{3.5}$$

Thus, $C^{\alpha\beta}(\mathbf{q}=\mathbf{0})$ is diagonal and not simply scalar as for a fcc crystal. Using Eqs. (3.4), (3.3), and (3.2) we derive

$$C^{xx}(\mathbf{q}=\mathbf{0})=C^{yy}(\mathbf{q}=\mathbf{0})\equiv C_1\ ,$$
$$C^{zz}(\mathbf{q}=\mathbf{0})=1-2C_1\equiv C_2\ . \tag{3.6}$$

We have supposed that the tetragonal axis at the muon site is parallel to the $\langle 001\rangle$ direction which is taken as the z axis. As the tetragonal axis can be parallel to either one of the three $\langle 100\rangle$ axes, there are three types of $C(\mathbf{q}=\mathbf{0})$ tensors for a given type of interstitial site. The diagonal elements are equal to (C_1,C_1,C_2), (C_1,C_2,C_1), or (C_2,C_1,C_1). A numerical computation gives $C_1=0.4541$ and $C_1=-0.0927$ for a tetrahedral and an octahedral interstitial site, respectively.

We notice that if the dipolar coupling between the muon magnetic moment and the lattice magnetic moments is restricted to the muon nearest-neighbor ions, the piecewise continuous behavior at $\mathbf{q}=0$ is not found.

Since $D^{\alpha\beta}(\mathbf{q}\to\mathbf{0})$ depends on the point symmetry at the muon site and therefore can be anisotropic, we infer that λ_z can have an anisotropic behavior even if the spin dynamics is isotropic.

Instead of performing the lattice sum for $D^{\alpha\beta}(\mathbf{q})$ we could have made a continuum approximation with the result[22]

$$D^{\alpha\beta}(\mathbf{q}\to 0)=-4\pi\left[\frac{q_\alpha q_\beta}{q^2}-\frac{1}{3}\delta^{\alpha\beta}\right]\ . \tag{3.7}$$

This approximation is not valid because it predicts that the $C(\mathbf{q}=\mathbf{0})$ tensor is always scalar. The breakdown of this approximation near $\mathbf{q}=\mathbf{0}$ is not surprising because the dipole sum is strongly dependent on the origin taken for the sum.[23]

Because the HI is of short range and isotropic, the $\mathbf{q}$ representation of the related tensor is easily obtained. In lowest order in $\mathbf{q}$ we have

$$H^{\alpha\beta}(\mathbf{q}=\mathbf{0})=r_\mu H\delta^{\alpha\beta}\ , \tag{3.8}$$

where r_μ is the number of nearest-neighbor magnetic ions to the muon localization site. Equation (3.8) is derived

under the hypothesis that the muon site is a center of symmetry.

IV. SPIN CORRELATION FUNCTIONS AT SMALL-q VECTOR FOR AN ISOTROPIC DIPOLAR CUBIC FERROMAGNET ABOVE T_C

Equation (2.20) shows that the μSR damping rate depends on symmetrized spin correlation functions of the magnet, $\tilde{\Lambda}^{\beta\gamma}(\mathbf{q})$. In this section we consider these functions.

Before discussing the properties of $\tilde{\Lambda}^{\beta\gamma}(\mathbf{q})$ we need to introduce the Hamiltonian $\mathcal{H}$ of the magnet which, in this work, we suppose to be an isotropic dipolar cubic ferromagnet. Below we discuss some of its properties. More details can be found elsewhere.[4,5,19] $\mathcal{H}$ writes

$$\mathcal{H}=-\sum_{i,j}{}' \mathcal{J}_{ij}\mathbf{J}_i\cdot\mathbf{J}_j + \frac{1}{2}\frac{\mu_0}{4\pi}\sum_{i,j}{}' \frac{(g_L\mu_B)^2}{(\mathbf{r}_i-\mathbf{r}_j)^3}\left[\mathbf{J}_i\mathbf{J}_j-3\frac{(\mathbf{J}_i\cdot\mathbf{r}_i)(\mathbf{J}_j\cdot\mathbf{r}_j)}{(\mathbf{r}_i-\mathbf{r}_j)^2}\right], \tag{4.1}$$

where $\mathcal{J}_{ij}$ is the exchange parameter between spins J_i and J_j, i.e., the interaction energy between these two spins is $2\mathcal{J}_{ij}$. $\sum'$ indicates that the term $i=j$ has to be omitted from the sum. Because in this paper we consider the magnet only above T_C, we have $\langle \delta\mathbf{J}_i\rangle=\mathbf{0}$, i.e., $\mathbf{J}_i=\delta\mathbf{J}_i$. We now perform a space-Fourier transform. For a cubic lattice, the Hamiltonian then becomes approximately

$$\mathcal{H}=\int\frac{vd^3q}{(2\pi)^3}\sum_{\alpha,\beta}\left[(-\mathcal{J}_0+\mathcal{J}\mathbf{q}^2a^2)\delta^{\alpha\beta}+\frac{c}{6}\mathcal{J}g\underline{D}^{\alpha\beta}(\mathbf{q}\delta)\right]J_\alpha(\mathbf{q})J_\beta(-\mathbf{q}), \tag{4.2}$$

where a is the lattice parameter (the cube edge) and δ the distance between a lattice site and one of its c nearest neighbors. We have retained terms only up to second order in $\mathbf{q}$ and have supposed that the exchange interaction extends up to the second nearest neighbors. For bcc and fcc lattices we have $\mathcal{J}=\mathcal{J}_1+\mathcal{J}_2$ where $\mathcal{J}_1$ and $\mathcal{J}_2$ are, respectively, the values of the exchange parameter between nearest neighbors and next-nearest neighbors. For a simple cubic (sc) crystal the relation is $\mathcal{J}=\mathcal{J}_1+4\mathcal{J}_2$. The parameter $\mathcal{J}_0=r_1\mathcal{J}_1+r_2\mathcal{J}_2$, where r_1 and r_2 are, respectively, the number of nearest and next-nearest neighbors, does not enter the spin equations of motion. The $\mathbf{q}$ representation of the dipolar interaction between the lattice magnetic moments in the limit of long wavelengths is represented by the tensor

$$\underline{D}^{\alpha\beta}(\underline{\mathbf{q}})=\frac{1}{a_1}\left\{a_1\frac{\underline{q}_\alpha\underline{q}_\beta}{\underline{q}^2}-a_2\underline{q}_\alpha\underline{q}_\beta-[a_3+a_4\underline{q}^2-a_5\underline{q}_\alpha^2]\delta^{\alpha\beta}\right\}, \tag{4.3}$$

where $\underline{\mathbf{q}}$ is a dimensionless wave vector and a_k, $k=1,2,\ldots,5$, are constants depending on the lattice structure.[19,24] The ratio of the dipolar to exchange interaction is characterized by the dimensionless parameter

$$g=(q_D\delta)^2 . \tag{4.4a}$$

Here the dipolar wave vector q_D is defined by

$$(q_Da)^2=\frac{\mu_0}{4\pi}\frac{a_1(g_L\mu_B)^2}{2\mathcal{J}\delta^3} . \tag{4.4b}$$

The a_1 and δ parameters depend on the lattice structure; see Table I.

TABLE I. Crystal structure dependent parameters of Bravais cubic lattices. c counts the number of next-nearest neighbors to a given lattice site. a_1 is defined at Eq. (4.3) and b at Eq. (4.14a). δ is the distance between nearest-neighbor ions and v the volume of the Bravais lattice primitive cell. a is the cube edge.

	sc	bcc	fcc
c	6	8	12
a_1	4π	$3\pi\sqrt{3}$	$4\pi\sqrt{2}$
b	1	$\sqrt{2}$	2
δ/a	1	$\sqrt{3}/2$	$\sqrt{2}/2$
v/a^3	1	$\frac{1}{2}$	$\frac{1}{4}$

For our study of the critical dynamics we have to retain in $\mathcal{H}$ only the terms relevant in the sense of the renormalization-group theory. This means that we only keep the first term in the expression of $\underline{D}^{\alpha\beta}(\underline{\mathbf{q}})$. The third and fourth terms are relevant but negligible in comparison to the terms of the same symmetry of the Heisenberg interaction. Therefore, the effective Hamiltonian to study the (paramagnetic) critical dynamics is given by

$$\mathcal{H}=\int\frac{vd^3q}{(2\pi)^3}\sum_{\alpha,\beta}\left[(-\mathcal{J}_0+\mathcal{J}\mathbf{q}^2a^2)\delta^{\alpha\beta}+\frac{c}{6}\mathcal{J}g\frac{q_\alpha q_\beta}{q^2}\right]J_\alpha(\mathbf{q})J_\beta(-\mathbf{q})$$
$$=\int\frac{vd^3q}{(2\pi)^3}\sum_{\alpha,\beta}\left[(-\mathcal{J}_0+\mathcal{J}\mathbf{q}^2a^2)P_{\mathrm{T}}^{\alpha\beta}(\mathbf{q})+\left[-\mathcal{J}_0+\mathcal{J}\mathbf{q}^2a^2+\frac{c}{6}\mathcal{J}g\right]P_{\mathrm{L}}^{\alpha\beta}(\mathbf{q})\right]J_\alpha(\mathbf{q})J_\beta(-\mathbf{q}), \tag{4.5}$$

where $P_{\mathrm{T}}^{\alpha\beta}(\mathbf{q})$ and $P_{\mathrm{L}}^{\alpha\beta}(\mathbf{q})$ are the transverse and longitudinal projection operators, respectively, i.e., $P_{\mathrm{T}}^{\alpha\beta}(\mathbf{q})=\delta^{\alpha\beta}-P_{\mathrm{L}}^{\alpha\beta}(\mathbf{q})$, where $P_{\mathrm{L}}^{\alpha\beta}(\mathbf{q})=q^\alpha q^\beta/q^2$. For further reference we notice that these operators obey the orthogonality relation

$$\sum_\beta P_{\mathrm{L}}^{\alpha\beta}(\mathbf{q})P_{\mathrm{T}}^{\beta\gamma}(\mathbf{q})=0 . \tag{4.6}$$

Writing $\mathcal{H}$ in terms of projector operators shows that it is the sum of two separate terms which describe the transverse (to $\mathbf{q}$) and longitudinal spin dynamics, respectively.

The symmetry property of $\mathcal{H}$ in $\mathbf{q}$ space allows one to write for the spin correlation function

$$\tilde{\Lambda}^{\beta\gamma}(\mathbf{q})=\tilde{\Lambda}^{\mathrm{T}}(q)P_{\mathrm{T}}^{\beta\gamma}(\mathbf{q})+\tilde{\Lambda}^{\mathrm{L}}(q)P_{\mathrm{L}}^{\beta\gamma}(\mathbf{q}) , \tag{4.7}$$

where $\tilde{\Lambda}^{\mathrm{T}}(q)$ and $\tilde{\Lambda}^{\mathrm{L}}(q)$ are the transverse and longitudinal correlation functions, respectively.

Instead of the correlation functions one can equivalently consider the static wave-vector-dependent susceptibilities $\chi^{\beta\gamma}(q)$ and the spectral weight functions $F^{\beta\gamma}(q,\omega)$. Notice that neutron-scattering experiments allow one to study these latter functions. Due to the fluctuation-dissipation theorem[25]

$$\tilde{\Lambda}^{\mathrm{T,L}}(q)=\frac{N}{\mu_0(g_L\mu_B)^2}k_BT\chi^{\mathrm{T,L}}(q)\tilde{F}^{\mathrm{T,L}}(q) , \tag{4.8}$$

all these functions are related to each other. (k_B is the Boltzmann constant.) The spectral weight function (or Kubo relaxation function), $F^{\mathrm{T,L}}(q,\omega)$, is reasonably well approximated by a Lorentzian as long as one is just interested in the width of the spectral weight function and not its form.[5] Thus, we can write

$$\tilde{F}^{\mathrm{T,L}}(q)=F^{\mathrm{T,L}}(q,\omega=0)=2/\Gamma^{\mathrm{T,L}}(q) , \tag{4.9}$$

where $\Gamma^{\mathrm{T,L}}(q)$ are, respectively, the transverse and longitudinal linewidths of the quasielastic peaks (Lorentzian functions of ω).

Only the transverse spin fluctuation parameter $\Gamma^{T}(q)$ can be studied by scattering of unpolarized neutrons. A separation of the longitudinal from the transverse susceptibilities can be achieved by the use of polarized neutrons.[26] Note that suitable experimental conditions are needed. For example, neutron measurements can only be performed for sufficiently large[3] q values, i.e., $q\gtrsim 0.01$ Å^{-1}. Introducing Eqs. (4.8) and (4.9) in Eq. (4.7) we derive

$$\tilde{\Lambda}^{\beta\gamma}(\mathbf{q})=\frac{2N}{\mu_0(g_L\mu_B)^2}k_BT\left[\frac{\chi^{\mathrm{T}}(q)}{\Gamma^{\mathrm{T}}(q)}P_{\mathrm{T}}^{\beta\gamma}(\mathbf{q})+\frac{\chi^{\mathrm{L}}(q)}{\Gamma^{\mathrm{L}}(q)}P_{\mathrm{L}}^{\beta\gamma}(\mathbf{q})\right] . \tag{4.10}$$

To make quantitative predictions we need to have information on the behavior of the $\chi^{\mathrm{L,T}}(q)$ and $\Gamma^{\mathrm{L,T}}(q)$ functions. We now first review the predictions of the critical scaling theory and then briefly describe the quantitative results recently obtained from mode-coupling (MC) theory.[4,5]

In the critical temperature regime the static susceptibilities and linewidths must obey scaling laws. One of the scaling lengths is the correlation length ξ as usual. The dipolar interaction introduces the second length scale q_D^{-1}. Hence, we have two scaling variables: $x=1/q\xi$ and $y=q_D/q$. As a consequence one gets an extension of the static scaling law

$$\chi^{\mathrm{L,T}}(q)=\Upsilon q^{-2}\hat{\chi}^{\mathrm{L,T}}(x,y) , \tag{4.11}$$

TABLE II. Material parameters for Ni, Fe, EuO, and EuS. The parameters are defined in the main text. Their values have been taken from the references mentioned in the table. When no reference is indicated, the parameter has been computed from a formula given in the main text with parameters given in Tables I and II.

	Ni	EuO	EuS	Fe
a (Å)	3.52 (Ref. 33)	5.12 (Ref. 34)	5.95 (Ref. 34)	2.87 (Ref. 33)
T_C (K)	627 (Ref. 33)	69.1 (Ref. 34)	16.6 (Ref. 34)	1043 (Ref. 33)
q_D (Å^{-1})	0.013 (Ref. 1)	0.147 (Refs. 1 and 35)	0.245 (Refs. 1 and 35)	0.045 (Ref. 35) [0.033 (Ref. 1)]
ξ_0 (Å)	1.23 (Ref. 38)	1.57 (Ref. 39)	1.81 (Ref. 39)	0.95 (Ref. 36) [0.82 (Ref. 37)]
$r_\mu H/4\pi$ ($T=0$ K)	−0.11 (Ref. 40)	0 (?)	0 (?)	−0.51 (Ref. 40)
Υ (Å)	0.00184	0.725	3.16	0.0239 (0.0129)
Ω_{expt} (meV Å$^{5/2}$)	350 (Ref. 38)	8.7 (Ref. 35) [8.3 (Ref. 42)]	2.1 (Ref. 43) [2.25 (Ref. 44)]	130 (Ref. 41)
Ω_{LOR} (meV Å$^{5/2}$)	241	7.09	2.08	90.0 (123)
$\mathcal{W}_{\mathrm{theor}}$ (MHz)	0.358	5.35 (5.60)	6.87 (6.41)	2.98 (2.56)

where $\hat{\chi}^{L,T}(x,y)$ are susceptibility scaling functions. Υ is a nonuniversal constant which is not given by the scaling theory. From MC theory one derives

$$\Upsilon=\frac{\mu_0(g_L\mu_B)^2}{2\mathcal{J}a^2} . \tag{4.12a}$$

The method we have followed to derive this latter formula for Υ is analogous to the one used in Appendix A of Ref. 27. Then Υ can be expressed in terms of the dipolar wave vector using Eq. (4.4b):

$$\Upsilon=\frac{4\pi q_D^2\delta^3}{a_1} . \tag{4.12b}$$

In Table II we have listed the Υ value of the four magnets we consider in this paper.

We can write scaling relations for the linewidths using the dynamical scaling law. We obtain

$$\hbar\Gamma^{L,T}(q)=\Omega q^z\hat{\Gamma}^{L,T}(x,y) , \tag{4.13}$$

with $z=\frac{5}{2}$. The nonuniversal frequency scale of Eq. (4.13) can be derived from MC theory. If the Lorentzian approximation mentioned at Eq. (4.9) is used, one obtains

$$\Omega_{\mathrm{Lor}}=\frac{P}{b}\sqrt{2\mathcal{J}k_BT_C/4\pi^4}a^{5/2} , \tag{4.14a}$$

where b is a dimensionless parameter which depends on the crystal structure (see Table I) and $P\cong 5.1326$. This latter parameter is chosen in such a way that the scaling functions are normalized to 1 at criticality and at $q_D=0$, i.e., $\hat{\Gamma}^{L,T}(x=0,y=0)=1$. A proof of Eq. (4.14) is given in Appendix B. Ω_{Lor} can be written in terms of the dipolar wave vector:

$$\Omega_{\mathrm{Lor}}=\frac{P}{\pi^{3/2}}\sqrt{\mu_0/4\pi}\frac{g_L\mu_B}{q_D}\sqrt{k_BT_C} . \tag{4.14b}$$

In Table II we list the Ω_{Lor} values computed from Eq. (4.14b) with $g_L=2$. A comparison between the experimental value Ω_{exp} and Ω_{Lor} shows that the energy scale of the fluctuations is qualitatively determined by the present MC theory. The largest difference is observed for Ni ($\simeq 30\%$). The crossover of the critical dynamical exponent is contained in the scaling linewidth functions $\hat{\Gamma}^{L,T}(x,y)$. When q is sufficiently small the linewidths $\Gamma^{L,T}(q,g)$ are proportional to $q^{z_{\mathrm{eff}}}$, where z_{eff} is an effective critical exponent. If the spin dynamics is driven by the Heisenberg interaction, i.e., when $q\gg q_D$, $z_{\mathrm{eff}}=\frac{5}{2}$ for the longitudinal as well as the transverse linewidths. In contrast, in the dipolar regime, i.e., $q\ll q_D$, z_{eff} is either equal to 0 or 2 depending on whether one refers to the longitudinal or transverse linewidth.

For a quantitative prediction of the damping rate we need to completely specify the susceptibility and the linewidth functions and not only their general behavior as given by the scaling theory.

We will use the Ornstein-Zernike forms for the susceptibilities

$$\chi^T(q)=\frac{\Upsilon}{q^2+\xi^{-2}}$$

and (4.15)

$$\chi^L(q)=\frac{\Upsilon}{q^2+q_D^2+\xi^{-2}} .$$

The correlation length ξ follows a power law:

$$\xi=\xi_0\left[\frac{T-T_C}{T_C}\right]^{-\nu} , \tag{4.16}$$

where ξ_0 is the critical amplitude. Notice that the Ornstein-Zernike forms are consistent with the MC approximation. We neglect Fisher's critical exponent η. This is legitimate for a three-dimensional Heisenberg magnetic system. The static critical exponents for the dipolar region are very close to the values for the exchange region. Therefore, we take $\nu\simeq\gamma/2$ with $\nu\simeq 1.37/2\simeq 0.69$. Equations (4.15) and (4.16) show that while the transverse susceptibility diverges at T_C when q goes to zero, the longitudinal susceptibility remains finite. These predictions have been checked for EuO and EuS by polarized neutron scattering.[28]

The influence of the dipolar interaction on the paramagnetic critical dynamics of cubic ferromagnets has been studied quantitatively on the basis of the MC theory.[4,5] Here, we would like to review shortly some of the basic assumptions. As a simple example of the application of the MC theory, we derive at Appendix B the integral equation obeyed by the linewidth $\Gamma(q)$ for the Heisenberg Hamiltonian.

In deriving the MC equations one starts from so-called generalized Langevin equations for the spectral weight functions[29,30] $F^\alpha(q,t)$. This leads to a set of two coupled integral equations ($\alpha=$L,T)

$$\frac{\partial F^\alpha(q,t)}{\partial t}=-\int_0^t d\tau M^\alpha(q,t-\tau)F^\alpha(q,\tau) , \tag{4.17}$$

where $M^\alpha(q,t)$ is a memory function. Due to the symmetry of the Hamiltonian, Eq. (4.5), it is necessary to decompose the spin operator $\mathbf{J}(\mathbf{q})$ into one longitudinal and two transverse components with respect to the wave vector $\mathbf{q}$. Then the memory functions is expressed in terms of scalar products (Kubo scalar product) of the time derivative of these components. The general structure of the Heisenberg equation for the longitudinal spin operator is

$$\frac{\partial J^L(\mathbf{q})}{\partial t}=\cdots[(\mathbf{q}\cdot(2\mathbf{k}-\mathbf{q})+\cdots q_D)\mathbf{J}^{T_1}(\mathbf{q}-\mathbf{k})J^{T_2}(\mathbf{k})] , \tag{4.18}$$

and for the transverse spin operators correspondingly. The terms proportional to the dipolar wave vector q_D result from the dipolar interaction in the Hamiltonian. In the limit $\mathbf{q}\to\mathbf{0}$ they remain finite, whereas all the other terms vanish. This reflects the fact that the dipolar interaction leads to a relaxation dynamics with a nonconserved order parameter in the limit of long wavelength.

The MC approximation amounts to neglecting a projection operator in the memory function and to performing factorization of the four-spin correlation functions that result from the insertion of the equations of motion, Eq. (4.18), in the memory function. (For a refined version of mode-coupling theory which allows for a consistent treatment of the Fisher exponent η and gives some justification for the above factorization procedure see Ref. 31). Physically this approximation means that one considers that a given mode decays into only two modes;[30] see Appendix B. This type of approximation has been found to be very successful in many areas of condensed-matter theory. In the present case it gives for the memory function

$$M^{\alpha}(q,t)\chi^{\alpha}(q)=2\left[\frac{2\mathcal{J}a^2}{\hbar}\right]^2\frac{k_BT}{\mu_0(g_L\mu_B)^2}\int\frac{vd^3k}{(2\pi)^3}\sum_{\beta,\sigma}v^{\alpha}_{\beta\sigma}(k,q,\eta)(\delta^{\sigma T}+\delta^{\alpha T}\delta^{\beta L}\delta^{\sigma L})$$
$$\times\chi^{\beta}(k)\chi^{\sigma}(|\mathbf{q}-\mathbf{k}|)F^{\beta}(k,t)F^{\sigma}(|\mathbf{q}-\mathbf{k}|,t)\ , \tag{4.19}$$

where the functions $v^{\alpha}_{\beta,\sigma}(k,q,\eta)$ describe the decay of mode α into modes β and σ (Refs. 4 and 5) and $\eta=\mathbf{q}\cdot\mathbf{k}/qk$. Notice that the memory, susceptibility, and spectral weight functions depend on the dipolar wave vector q_D. These coupled MC equations [Eqs. (4.17) and (4.19)] obey generalized dynamical scaling laws.[4] If one is not interested in the precise frequency dependence of the correlation functions, it is a quite reasonable approximation to assume that the memory kernel $M^{\alpha}(q,t)$ decays much faster in time than the Kubo relaxation function $F^{\alpha}(q,t)$ in Eq. (4.17). Hence the Lorentzian linewidth can be written as

$$\Gamma^{\alpha}(q)=\int_0^{\infty}dt\,M^{\alpha}(q,t)\ . \tag{4.20}$$

Note that this approximation, which is equivalent with the Lorentzian approximation used in Eq. (4.9), can be justified by studying the frequency dependence of the correlation functions[5] and the resulting linewidths. This additional approximation finally leads to a simplified set of coupled integral equations for the transverse and longitudinal linewidths which obey the generalized scaling law, Eq. (4.13).

The main results derived from these MC equations are as follows.[4,5] At the critical temperature T_C there is a crossover in the effective dynamical critical exponent from $z_{\text{eff}}=2.5$ to 2.0 for the transverse and to $z_{\text{eff}}=0$ for the longitudinal linewidth. This is expected from scaling theory as noticed after Eqs. (4.14). But, whereas the crossover for the longitudinal linewidth occurs in the immediate vicinity of the dipolar wave vector, the crossover in the transverse linewidth is shifted to a wave vector which is almost one order of magnitude smaller. This last quantitative result is only obtained from MC theory. Above the critical temperature one gets, as a function of the scaling variable x, a set of curves for the linewidth, which are parametrized by the product $q_D\xi$, i.e., the temperature. The deviation of these curves from the isotropic (Heisenberg) result becomes larger as one is approaching the critical temperature. These predictions have been confirmed experimentally for the transverse as well as the longitudinal linewidth.[3,26] Furthermore, the frequency dependence has also been analyzed within MC theory[5] and agrees with neutron-scattering experiments.[26,32]

For the relaxation rate of the homogeneous magnetization, which can be observed in ESR and magnetic relaxation experiments, the dipolar interaction leads to a crossover from a "critical speeding up" in the isotropic (Heisenberg) region to a thermodynamic slowing down in the dipolar limit. As it has been reviewed recently, the theoretical results are in quantitative agreement with experiment.[1]

Applying the MC theory to hyperfine-interaction experiments with a short-range interaction (like PAC), one finds[4] that the autocorrelation time τ_C diverges like $\tau_C\propto\xi$ corresponding to an effective dynamic exponent $z_{\text{eff}}=2$ in the asymptotic dipolar region. Upon leaving the asymptotic region there is a crossover to the isotropic Heisenberg region, where $\tau_C\propto\xi^{3/2}$ corresponding to $z_{\text{eff}}=2.5$. As in the above cases the predicted scaling function[4] for the autocorrelation time is in quantitative agreement with experimental data on Fe and Ni.[2] In the next section we will study the case of μSR, where, in contrast to PAC, the interaction between the muon and the material is no longer only short ranged.

V. PREDICTION FOR THE ZERO-FIELD μSR DEPOLARIZATION RATE OF ISOTROPIC DIPOLAR PARAMAGNETS NEAR T_C

Using the information given in the previous sections, we can compute the damping rate λ_z for specified magnets. But before doing it, we present some general results.

We recall that in this paper we consider the muon-lattice coupling tensor $G(\mathbf{q})$ only in lowest order in $\mathbf{q}$. We first neglect the muon dipolar interaction and consider the case of a pure contact interaction. Thus we have

$$G^{\alpha\beta}(\mathbf{q}=\mathbf{0})=H^{\alpha\beta}(\mathbf{q}=\mathbf{0})=r_{\mu}H\delta^{\alpha\beta}\ ,$$

see Eq. (3.8). Using Eqs. (2.20) and (4.10) we obtain

$$\lambda_z=\frac{\mu_0}{4\pi}\frac{(\gamma_{\mu}r_{\mu}H)^2}{2}\frac{k_BT}{v}$$
$$\times\int\frac{d^3\mathbf{q}}{(2\pi)^3}\left[\frac{\chi^{\mathrm{T}}(q)}{\Gamma^{\mathrm{T}}(q)}\left[1+\frac{q_z^2}{q^2}\right]+\frac{\chi^{\mathrm{L}}(q)}{\Gamma^{\mathrm{L}}(q)}\left[1-\frac{q_z^2}{q^2}\right]\right]\ . \tag{5.1}$$

Because the susceptibility and linewidth functions depend only on q, the integral over the angles ($\int d\mathbf{q}^3$

$=\int_0^{q_{BZ}} dq\, q^2 \int_0^{\pi} d\theta \sin\theta \int_0^{2\pi} d\psi$) can be performed. We obtain

$$\lambda_z = \frac{1}{6\pi^2}\frac{\mu_0}{4\pi}(\gamma_\mu r_\mu H)^2 \frac{k_B T}{v} \times \int_0^{q_{BZ}} dq\, q^2 \left[2\frac{\chi^T(q)}{\Gamma^T(q)} + \frac{\chi^L(q)}{\Gamma^L(q)} \right] . \quad (5.2)$$

We have approximated the Brillouin zone by a sphere of radius q_{BZ}. If the dipolar interaction between the magnetic ions is negligible, Eq. (5.2) reduces to

$$\lambda_z = \frac{1}{2\pi^2}\frac{\mu_0}{4\pi}(\gamma_\mu r_\mu H)^2 \frac{k_B T}{v} \int_0^{q_{BZ}} dq\, q^2 \frac{\chi(q)}{\Gamma(q)} , \quad (5.3)$$

where $\chi(q)$ and $\Gamma(q)$ are, respectively, the static wave-vector susceptibility and linewidth functions for the Heisenberg (isotropic) Hamiltonian. Using the scaling laws for these two functions we get, when the temperature is sufficiently close to T_C, the power-law relation[2]

$$\lambda_z = \mathcal{U}\left[\frac{T - T_C}{T_C} \right]^{-w} , \quad (5.4a)$$

with the nonuniversal constant $\mathcal{U}$ given by

$$\mathcal{U} = \frac{1}{2\pi^2}\frac{\mu_0}{4\pi}(\gamma_\mu r_\mu H)^2 \xi_0^{z-1} \frac{\hbar\Upsilon}{\Omega}\frac{k_B T}{v} \times \int_0^{\infty} dx\, x^{z-2} \frac{\hat{\chi}(x, y=0)}{\hat{\Gamma}(x, y=0)} , \quad (5.4b)$$

with $z = \frac{5}{2}$.

The exponent is $w = \nu(z-1)$. Because we are only interested in a limited temperature range above T_C, T can be safely replaced by T_C in Eq. (5.4b). Equation (5.4a) indicates that the value of z can be derived from an analysis of the temperature dependence of the damping rate. When the dipolar interaction between the ion magnetic dipoles cannot be neglected, it is still possible to analyze the data using Eq. (5.4a) in restricted temperature ranges. Then one gets effective dynamic exponents which have direct physical meaning.[2] But, as shown below, in μSR spectroscopy it may be essential to properly take into account the effect of the muon-lattice dipolar interaction if one wants to extract reliable information from the data.

We now consider the case where the muon magnetic moment interacts with the lattice ion magnetic moments through the dipolar and contact interactions. We first suppose that the tensor $C(\mathbf{q}=\mathbf{0})$ is scalar as found for a muon in a fcc crystal. Then the coupling tensor near $\mathbf{q}=\mathbf{0}$ is written (see Sec. III):

$$G^{\alpha\beta}(\mathbf{q}\to\mathbf{0}) = -4\pi\left[\frac{q_\alpha q_\beta}{q^2} - \frac{1}{3}\delta^{\alpha\beta} \right] + r_\mu H \delta^{\alpha\delta} . \quad (5.5)$$

From this result we derive

$$\lambda_z = \frac{8}{3}\frac{\mu_0}{4\pi}\gamma_\mu^2 \frac{k_B T}{v} \times \int_0^{q_{BZ}} dq\, q^2 \left[2p^2 \frac{\chi^T(q)}{\Gamma^T(q)} + (1-p)^2 \frac{\chi^L(q)}{\Gamma^L(q)} \right] , \quad (5.6a)$$

where we have defined

$$p = \frac{1}{3} + \frac{r_\mu H}{4\pi} . \quad (5.6b)$$

We have used the $\tilde{\Lambda}^{\beta\gamma}(\mathbf{q})$ expression from Eq. (4.10) and the orthogonality property of the projection operators given at Eq. (4.6). When the Fermi contact interaction is large compared to the classical dipolar interaction, i.e., $|p| \gg 1$, Eq. (5.6a) reduces to Eq. (5.2) as expected.

On the other hand, when the Fermi interaction is negligible, i.e., $p \simeq \frac{1}{3}$, we get from Eq. (5.6a)

$$\lambda_z = \frac{16}{27}\frac{\mu_0}{4\pi}\gamma_\mu^2 \frac{k_B T}{v} \int_0^{q_{BZ}} dq\, q^2 \left[\frac{\chi^T(q)}{\Gamma^T(q)} + 2\frac{\chi^L(q)}{\Gamma^L(q)} \right] . \quad (5.7)$$

While Eq. (5.2) has been derived with the hypothesis that the muon spin interacts with the lattice spins through the isotropic hyperfine interaction, Eq. (5.7) has been obtained supposing that the coupling is only due to the classical dipolar interaction. The origin of the relative weight (2:1) of the transverse modes compared to the longitudinal modes in Eq. (5.2) is obvious. When the muon dipolar interaction dominates [Eq. (5.5) with $H=0$], the relative weight of the modes is inverted; see Eq. (5.7). This can be understood by counting the modes. The contribution of the $\delta^{\alpha\beta}/3$ factor is $\frac{2}{3}$ from the transverse modes and $\frac{1}{3}$ from the longitudinal modes. The $q^\alpha q^\beta/q^2$ term is only coupled to the longitudinal modes. Therefore, its weight factor is one longitudinal mode. Hence all together this counting of modes predicts that when the interaction is purely dipolar, there are twice more longitudinal modes coupled to the muon magnetic moment than transverse modes. This is exactly the prediction made by Eq. (5.7).

For the numerical integration of Eq. (5.6a) it is convenient to introduce polar coordinates

$$r = (x^2 + y^2)^{1/2}$$

and (5.8)

$$\varphi = \arctan(y/x) ,$$

where x and y are the scaling variables defined previously. We notice that the angle φ is a measure for the temperature:

$$\varphi = \arctan(q_D \xi) . \quad (5.9)$$

Using these new two variables we derive

$$\lambda_z = \mathcal{W}\left[1 + \frac{1}{(q_D\xi)^2} \right]^{-3/4} \times \int_{r_0}^{\infty} dr\, r^{1/2} \left[2p^2 \frac{\hat{\chi}^T(r,\varphi)}{\hat{\Gamma}^T(r,\varphi)} + (1-p)^2 \frac{\hat{\chi}^L(r,\varphi)}{\hat{\Gamma}^L(r,\varphi)} \right] , \quad (5.10a)$$

where the nonuniversal constant $\mathcal{W}$ is given by

$$\mathcal{W}=\frac{8}{3}\frac{\mu_0}{4\pi}\frac{\gamma_\mu^2}{q_D^{3/2}}\frac{\hbar\Upsilon}{\Omega}\frac{k_BT}{v}\simeq\frac{8}{3}\frac{\mu_0}{4\pi}\frac{\gamma_\mu^2}{q_D^{3/2}}\frac{\hbar\Upsilon}{\Omega}\frac{k_BT_C}{v}\ . \tag{5.10b}$$

Using Eqs. (4.12b) and (4.14b) it is possible to give an expression of $\mathcal{W}$ which does not refer to Υ and Ω:

$$\mathcal{W}=\frac{8\pi^{3/2}}{3P}\sqrt{\mu_0/4\pi}\frac{\gamma_\mu^2\hbar q_D^{3/2}}{g_L\mu_B}\sqrt{k_BT_C}\ . \tag{5.10c}$$

The theoretical value of $\mathcal{W}$ for each of the four magnets considered in this paper is listed in Table II. The calculations have been performed using Eq. (5.10b) with the energy scale constant given by Ω_{expt}. A computation of $\mathcal{W}$ from Eq. (5.10c) gives values which are compatible with the former ones, taking into account the material parameter uncertainties. The lower cutoff r_0 is

$$r_0=\frac{\sqrt{q_D^2+\xi^{-2}}}{q_{\text{BZ}}}\ . \tag{5.10d}$$

It can be taken as 0 in the critical region.

Following Frey and Schwabl [Ref. 4, Z. Phys. B **71**, 355 (1988)], we define the functions

$$I^{\text{L,T}}(\varphi)=\left[1+\frac{1}{(q_D\xi)^2}\right]^{-3/4}\int_{r_0}^{\infty}dr\,r^{1/2}\frac{\hat{\chi}^{\text{L,T}}(r,\varphi)}{\hat{\Gamma}^{\text{L,T}}(r,\varphi)}\ . \tag{5.11}$$

With these functions, which are presented in Fig. 10 of Ref. 4 (with the lower cutoff set to 0), Eq. (5.10a) reduces to

$$\lambda_z=\mathcal{W}[2p^2I^{\text{T}}(\varphi)+(1-p)^2I^{\text{L}}(\varphi)]\ . \tag{5.12}$$

Figure 10 of Ref. 4 indicates that while $I^{\text{T}}(\varphi)$ exhibits a strong temperature dependence in the whole temperature range of the critical region, $I^{\text{L}}(\varphi)$ is practically temperature independent for $q_D\xi>1$. Therefore, the temperature dependence of the μSR damping rate λ_z depends on the relative weight of $I^{\text{T}}(\varphi)$ and $I^{\text{L}}(\varphi)$ which is controlled by the parameter p. As has been pointed out by Yushankhai,[11] the transverse fluctuations do not contribute to λ_z if $r_\mu H/4\pi=-\frac{1}{3}$. In this case λ_z becomes temperature independent near T_C. Using the previous equation we are now going to plot $\lambda_z(T)$ for different physical cases.

In Fig. 2 we present the experimental data of Nishiyama *et al.*[8] for metallic Ni. The solid line shows the temperature dependence given by Eq. (5.12) with $\mathcal{W}_{\text{expt}}=0.30$ MHz. The other parameters are listed in Tables I and II. We have used the $I^{\text{L,T}}(\varphi)$ functions computed from the MC theory.[4] It is rewarding that the $\mathcal{W}_{\text{expt}}$ and $\mathcal{W}_{\text{theor}}$ values agree within $\simeq 20\%$. Notice that there is no adjustable parameter for the temperature variable. The dashed line shows the prediction made by Eq. (5.2) which neglects the effect of the muon-lattice dipolar interaction. The nonuniversal parameter $\mathcal{U}$ has been chosen in such a way that the dashed and solid lines coincide at high temperature. It is obvious that it is important to take into account the muon dipolar interaction.

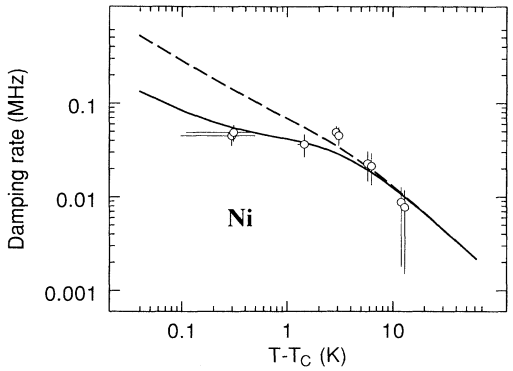

FIG. 2. Temperature dependence of the μSR damping rate for metallic Ni. The points are the experimental data of Nishiyama *et al.* (Ref. 8). The solid line is the result of the model which takes the muon dipolar interaction into account. The dashed line gives the prediction when this latter interaction is neglected.

In Fig. 3 are presented our predictions for EuO and EuS. We have used the parameters given in Table II. We have taken $\mathcal{W}_{\text{theor}}=5.35$ and 6.87 MHz for EuO and EuS, respectively. A comparison with experimental data is not possible because, up to now, no such data have been reported.

The shape of the $\lambda_z(T)$ functions shown in Figs. 3 and 2 are strongly different mainly because of the effect of the interference between the hyperfine interaction and the muon dipolar interaction for Ni. This leads to a small value for p and therefore to a small contribution of the transverse fluctuations to λ_z at moderate low temperatures. At temperatures close to T_C, $(T-T_C)<0.3$ K, λ_z is predicted to increase rapidly when going down in temperature. This behavior is produced by the transverse fluctuations which contribute significantly to the damping when approaching the Curie temperature. It would be interesting to have experimental data to check that prediction.

We now consider the case of a muon in a bcc crystal.

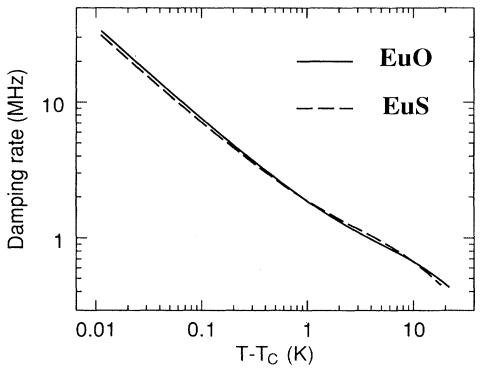

FIG. 3. Temperature dependence of the μSR damping rate for EuO and EuS predicted by mode-coupling theory. The theory presented in this paper has been built to describe the critical dynamics of paramagnets. Therefore, its predictions for relative temperature $(T-T_C)/T_C\gtrsim 0.1$ may be questionable.

Then the coupling tensor near $\mathbf{q}=\mathbf{0}$ for a given site is written (see Sec. III):

$$G^{\alpha\beta}(\mathbf{q}\to\mathbf{0})=-4\pi\left[\frac{q_\alpha q_\beta}{q^2}-d_\alpha\delta^{\alpha\beta}\right]+r_u H\delta^{\alpha\beta}\ . \tag{5.13}$$

From this result we derive

$$\lambda_z=\mathcal{W}\{(p_x^2+p_y^2)I^{\mathrm{T}}(\varphi) +\tfrac{1}{2}[(1-p_x)^2+(1-p_y)^2]I^{\mathrm{L}}(\varphi)\}\ , \tag{5.14a}$$

with

$$p_\alpha=d_\alpha+\frac{r_\mu H}{4\pi}\ . \tag{5.14b}$$

In metallic Fe the muon diffuses between magnetically inequivalent interstitial sites (in Ni the sites are all magnetically equivalent). We will suppose that the muon diffuses either between the tetrahedral or octahedral sites. In a first approximation we take the diffusion into account by performing an ensemble average over the damping rates corresponding to the different possible sites. Thus we have

$$\lambda_z=\tfrac{1}{3}(\lambda_z^{(1)}+\lambda_z^{(2)}+\lambda_z^{(3)})\ . \tag{5.15}$$

The Fe damping rate can now be computed from the previous equation with the help of Eq. (5.13a) and the C_1 coefficient given in Sec. III. We obtain

$$\lambda_z=\frac{\mathcal{W}}{3}\{[4s_1^2+2s_2^2]I^{\mathrm{T}}(\varphi) +[2(1-s_1)^2+(1-s_2)^2]I^{\mathrm{L}}(\varphi)\}\ , \tag{5.16a}$$

where we define

$$s_1=C_1+\frac{r_\mu H}{4\pi}$$

and

$$s_2=1-2C_1+\frac{r_\mu H}{4\pi}\ . \tag{5.16b}$$

In Figs. 4(a) and 4(b) we present a comparison between data recorded on metallic Fe and the theory developed in this paper. The experimental points are from Herlach *et al.*[9] In Fig. 4(a) [4(b)] we suppose that the muon diffuses between tetrahedral [octahedral] interstitial sites. There are two sets of material parameters; see Table II. For each figure, the dashed and solid lines are the result of the theory with (q_D,ξ_0) equal to (0.045 Å^{-1}, 0.95 Å) and (0.033 Å^{-1}, 0.82 Å), respectively. In the case of the muon diffusing between tetrahedral sites, the value of the nonuniversal constant $\mathcal{W}_{\mathrm{expt}}$ used for the fit is equal to 1.40 MHz for the first set of material parameters and to 2.50 MHz for the second set. In the case of the muon diffusing between octahedral sites, the nonuniversal constant $\mathcal{W}_{\mathrm{expt}}$ is found to be equal to 0.85 MHz for the first set and to 1.55 MHz for the second set of parameters. We observe that the second set of parameters gives a better fit. Furthermore, a comparison between Figs. 4(a) and 4(b) seems to indicate that the muon diffuses between octahedral sites. For a definite statement more data are needed, particularly near T_C. Equation (5.10b) predicts two theoretical values for the frequency scale depending on the (q_D,ξ_0) value. The values are listed in Table II. For the octahedral site, $\mathcal{W}_{\mathrm{theor}}$ (2.56 MHz) is larger than $\mathcal{W}_{\mathrm{expt}}$ (1.55 MHz) by $\simeq 40\%$. This disagreement between theory and experiment may not be surprising if one considers that for Fe the material parameters do not seem to be well determined (there are two sets of these parameters). In fact, the μSR data give a constraint on them. As for the case of Ni there is no adjustable parameter for the temperature variable. We notice that most of the data have been recorded in the crossover temperature region where λ_z is not predominantly due to the transverse fluctuations. Therefore, the meaning of the analysis of the data with a power law[9] such as given by Eq. (5.4a) is questionable. The data have been recorded with the transverse geometry. In a cubic metal such as Fe, the transverse field damping rate and the zero-field damping rate should be equal if the applied field is sufficiently large.[15] This is probably the case for the data of Herlach *et al.*[9] Therefore, the comparison made in Figs. 4(a) and 4(b) between the data and the theory is meaningful.

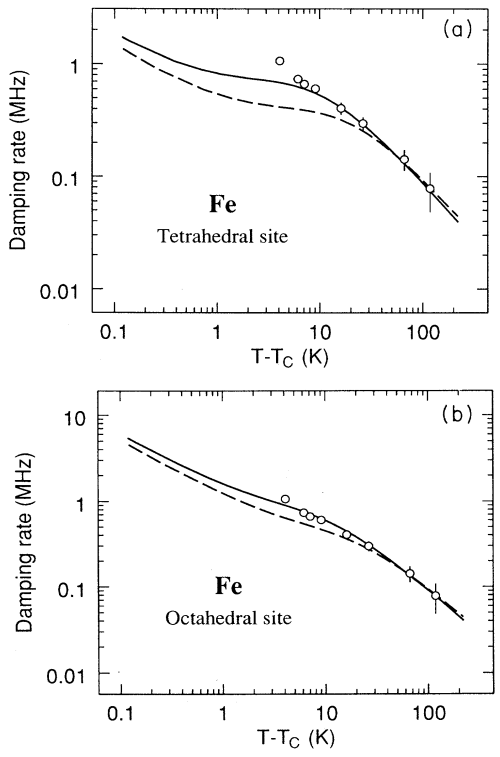

FIG. 4. Temperature dependence of the μSR damping rate for metallic Fe. The points are the experimental data of Herlach *et al.* (Ref. 9). The curves are the predictions of mode-coupling theory for different sets of material parameters. In (a) [(b)] the muon is supposed to diffuse between tetrahedral (octahedral) sites. The solid and dashed lines show the results obtained with (q_D,ξ_0) equal to (0.033 Å^{-1}, 0.82 Å) and to (0.045 Å^{-1}, 0.95 Å), respectively; see Table II.

VI. SUMMARY AND CONCLUSION

In this paper we have established the relation between the μSR zero-field damping rate and the susceptibility and spectral weight functions of a magnet. This has led us to study in detail the interaction between the muon magnetic moment and the lattice ion magnetic moments. We have given a formula for the **q** representation of that interaction. Because of the long-range nature of the classical dipolar interaction, it is not sufficient for a ferromagnet to only consider the nearest-neighbor ions to the muon.

We have reviewed the predictions made by the scaling theory and the mode-coupling theory for the critical dynamics properties above the Curie temperature of a Heisenberg dipolar ferromagnet. This has allowed us to define the parameters and to examine the hypotheses made by these theories.

Using mode-coupling theory we have been able to explain the paramagnetic critical behavior of the μSR damping rate published for metallic Fe and Ni. With previously determined material parameters, we have computed the nonuniversal constant $\mathcal{W}$ only within $\simeq 20\%$ for Ni ($\simeq 40\%$ for Fe). This slight discrepancy may be explained by the uncertainties on the material parameter values. In fact, the μSR data may give a constraint on these values. We have accounted well for the crossover behavior as the critical temperature is approached. We have made predictions for EuO and EuS. Our results show that the interference between the hyperfine coupling interaction and the muon dipolar interaction has a strong effect on the measured damping rate.

Our analysis seems to indicate that the muon diffuses in Fe between octahedral sites when $T \approx T_C$. Because the hyperfine field coupling constant is practically the same at T_C and at low temperature,[11] we have some indication that the muon site is the same at low and high temperature.

μSR spectroscopy can be very useful to study the critical spin dynamics of ferromagnets because the measurements can be performed in zero external field (therefore there is no problem with demagnetization field) and on any compound (the probe is implanted in the sample). It is now possible to analyze μSR data using the theoretical framework presented in this paper. Therefore quantitative information on the magnetic properties of the compound can be obtained.

Very interesting μSR data exist on metallic Gd.[10] They cannot be analyzed with the theoretical framework presented here because this metal has a non-Bravais and nonorthogonal crystal structure. It would be very useful to generalize the present work for such crystal structures.

ACKNOWLEDGMENTS

It is a pleasure to acknowledge helpful discussions with F. Schwabl. One of us (E.F.) acknowledges support from a grant from the Deutsche Forschungsgemeinschaft. This work was also supported by the National Science Foundation, through Grant No. DMR-91-15491 and through the Harvard Materials Research Laboratory.

APPENDIX A: *q* REPRESENTATION OF THE DIPOLAR TENSOR

The purpose of this appendix is to calculate

$$D^{\alpha\beta}(\mathbf{q}) = \sum_i D^{\alpha\beta}_{\mathbf{r}_i} \exp(i\mathbf{q}\cdot\mathbf{r}_i)$$
$$= \exp(i\mathbf{q}\cdot\mathbf{r}_0) v \sum_{\mathbf{i}} \left[\frac{\partial^2}{\partial r_\alpha \partial r_\beta} \frac{1}{|\mathbf{r}|} \right]_{\mathbf{r}=\mathbf{r}_i} \exp(i\mathbf{q}\cdot\mathbf{i}) , \tag{A1}$$

where we have used the identity $\mathbf{r}_i = \mathbf{r}_0 + \mathbf{i}$ (see Fig. 1). The sum runs over all the direct lattice sites.

We notice that

$$\left[\frac{\partial^2}{\partial r_\alpha \partial r_\beta} \frac{1}{|\mathbf{i}-\mathbf{x}|} \right]_{\mathbf{x}=-\mathbf{r}_0} = \left[\frac{\partial^2}{\partial r_\alpha \partial r_\beta} \frac{1}{|\mathbf{r}|} \right]_{\mathbf{r}=\mathbf{r}_i} . \tag{A2}$$

Therefore, as a first step towards the evaluation of (A1), we study $\sum_{\mathbf{i}} (1/|\mathbf{i}-\mathbf{x}|) \exp(i\mathbf{q}\cdot\mathbf{i})$. We follow Ewald's method.[18,19] Using the identity

$$\frac{1}{|\mathbf{i}-\mathbf{x}|} = \frac{2}{\sqrt{\pi}} \int_0^\infty d\rho \exp(-|\mathbf{i}-\mathbf{x}|^2\rho^2) , \tag{A3}$$

we can write

$$\sum_{\mathbf{i}} \frac{1}{|\mathbf{i}-\mathbf{x}|} \exp(i\mathbf{q}\cdot\mathbf{i}) = \int_0^\rho d\rho \left\{ \frac{2}{\sqrt{\pi}} \sum_{\mathbf{i}} \exp[-|\mathbf{i}-\mathbf{x}|^2\rho^2 + i\mathbf{q}\cdot(\mathbf{i}-\mathbf{x})] \right\} \exp(i\mathbf{q}\cdot\mathbf{x})$$
$$+ \sum_{\mathbf{i}} \left\{ \frac{2}{\sqrt{\pi}} \int_\rho^\infty d\rho \exp(-|\mathbf{i}-\mathbf{x}|^2\rho^2) \right\} \exp(i\mathbf{q}\cdot\mathbf{i}) . \tag{A4}$$

Following Ewald, we have divided the integrals into two regions: from 0 to ρ and from ρ to ∞. Now the expression in brackets ($\{ \cdots \}$) in the first term is a function of **x** with the lattice periodicity. Hence it can be expressed as a Fourier sum over the **K** vectors of the reciprocal lattice.[18,19] We then easily derive

$$\sum_{\mathbf{i}} \frac{1}{|\mathbf{i}-\mathbf{x}|} \exp(i\mathbf{q}\cdot\mathbf{i}) = \frac{4\pi}{v q^2} \exp\left[\frac{-q^2}{4\rho^2} \right] \exp(i\mathbf{q}\cdot\mathbf{x}) + \frac{\pi}{v\rho^2} \sum_{\mathbf{K}(\neq 0)} \varphi_0 \left[\frac{(\mathbf{K}+\mathbf{q})^2}{4\rho^2} \right] \exp[i(\mathbf{K}+\mathbf{q})\cdot\mathbf{x}]$$
$$+ \frac{\rho}{\sqrt{\pi}} \sum_{\mathbf{i}} \varphi_{-1/2}(\rho^2|\mathbf{i}-\mathbf{x}|^2) \exp(i\mathbf{q}\cdot\mathbf{i}) , \tag{A5}$$

where v is the volume of the Bravais lattice primitive cell. We have used the functions introduced by Misra:[20]

$$\varphi_m(x)=\int_1^\infty d\beta\,\beta^m \exp(-\beta x)\ . \tag{A6}$$

These functions have the following useful transformation properties:

$$\varphi_m(x)=\varphi_0(x)+(m/x)\varphi_{m-1}(x)\ , \tag{A7}$$

$$\frac{\partial}{\partial_x}\varphi_m(x)=-\varphi_{m+1}(x)\ . \tag{A8}$$

The second and final step towards the derivation of $D^{\alpha\beta}(\mathbf{q})$ is made by taking the derivatives of (A5) with respect to components of $\mathbf{x}$ [with the help of Eq. (A8)] and then setting $\mathbf{x}=-\mathbf{r}_0$. In addition, Eq. (A1) has to be used. The result is given at Eq. (3.1) of the main text.

APPENDIX B: COMPUTATION OF THE Ω CONSTANT

The purpose of this appendix is to compute from the mode-coupling theory the nonuniversal energy scale constant defined by Eq. (4.13). Especially, we want to scrutinize its dependence on the lattice structure. The energy scale constant can be computed by considering only the Heisenberg part of the Hamiltonian given at Eq. (4.2). The effect of the dipolar interaction is included in the scaling function $\hat{\Gamma}^{L,T}(x,y)$.

First we are going to compute an expression for the memory function of a Heisenberg system. The equivalent equation for the full dipolar Hamiltonian [Eq. (4.2)] is given in Eq. (4.19). Upon using the Lorentzian approximation, Eq. (4.20), we will derive an integral equation for the linewidth. The solution of this equation at $T=T_C$ will give us the formula for the energy scale.

In the MC approximation the memory function is related to the susceptibility function and the Kubo scalar product as follows:[30]

$$M^{xx}(\mathbf{q},t)=\frac{\mu_0(g_L\mu_B)^2}{N}\frac{(\dot{J}_x(\mathbf{q},t),\dot{J}_x(-\mathbf{q}))}{\chi^{xx}(\mathbf{q})}\ , \tag{B1}$$

where the dot over a spin variable stands for its time derivative. The time evolution of $J_x(\mathbf{q},t)$ can be computed from the Heisenberg equation. One obtains

$$\dot{J}_x(\mathbf{q},t)=\frac{2\mathcal{J}a^2}{\hbar}\int\frac{v\,dk^3}{(2\pi)^3}(2\mathbf{k}\cdot\mathbf{q}-q^2)J_y(\mathbf{k},t)J_z(\mathbf{q}-\mathbf{k},t)\ . \tag{B2}$$

Inserting the equations of motion, Eq. (B2), in Eq. (B1) we get

$$M^{xx}(\mathbf{q},t)=\frac{\mu_0(g_L\mu_B)^2}{N\chi^{xx}(\mathbf{q})}\frac{4\mathcal{J}^2a^4}{\hbar^2}\int\frac{v\,d^3k}{(2\pi)^3}\int\frac{v\,d^3k'}{(2\pi)^3}(2\mathbf{k}\cdot\mathbf{q}-q^2)(2\mathbf{k}'\cdot\mathbf{q}-q^2)(J_y(\mathbf{k},t)J_z(\mathbf{k}-\mathbf{q},t),J_y(-\mathbf{k}')J_z(\mathbf{k}'-\mathbf{q}))\ . \tag{B3}$$

Following the mode-coupling method, we decouple the four-point scalar product as follows:

$$(J_y(\mathbf{k},t)J_z(\mathbf{q}-\mathbf{k},t),J_y(-\mathbf{k}')J_z(\mathbf{k}'-\mathbf{q}))=\mathbf{k}_BT(J_y(\mathbf{k},t),J_y-\mathbf{k}'))(J_z(\mathbf{q}-\mathbf{k},t),J_z(\mathbf{k}'-\mathbf{q}))\delta_{\mathbf{k},\mathbf{k}'}\ . \tag{B4}$$

Due to rotational symmetry in spin space all physical quantities are independent of the Cartesian components. Therefore, we drop the Cartesian index. A two-point Kubo scalar product can be expressed in terms of a susceptibility and a spectral weight functions as follows:

$$(J_y(\mathbf{k},t),J_y(-\mathbf{k}))=\frac{N}{\mu_0(g_L\mu_B)^2}\chi_{\mathbf{k}}F_{\mathbf{k}}(t)\ . \tag{B5}$$

Combining Eqs. (B5), (B4), and (B3) we derive the equation obeyed by the memory function:

$$M(q,t)=2\left[\frac{2\mathcal{J}a^2}{\hbar}\right]^2\frac{k_BT}{\mu_0(g_L\mu_B)^2}\frac{1}{\chi(q)}\times\int\frac{v\,d^3k}{(2\pi)^3}v(k,q,\eta)\chi(k)\chi(|\mathbf{q}-\mathbf{k}|)\times F(k,t)F(|\mathbf{q}-\mathbf{k}|,t)\ , \tag{B6a}$$

where the vertex function is

$$v(k,q,\eta)=2\left[kq\eta-\frac{q^2}{2}\right]^2,\quad \eta\equiv\frac{\mathbf{q}\cdot\mathbf{k}}{qk}\ . \tag{B6b}$$

Notice that, due to rotational invariance in coordinate space, the memory, susceptibility, the spectral weight functions just depend on $k=|\mathbf{k}|$.

Using Eq. (4.20) the integral equation for the linewidth function can be deduced from the equation of the memory function we have just derived. In addition one has to remember that Eq. (4.20) implies that the spectral weight function is an exponential function in time space with the linewidth as the damping rate. Then the integral equation for the linewidth reads

$$\Gamma(q)=2\left[\frac{2\mathcal{J}a^2}{\hbar}\right]^2\frac{k_BT}{\mu_0(g_L\mu_B)^2}\frac{1}{\chi(q)}\times\int\frac{v\,d^3k}{(2\pi)^3}v(k,q,\eta)\chi(k)\chi(|\mathbf{q}-\mathbf{k}|)\times\frac{1}{\Gamma(k)+\Gamma(|\mathbf{q}-\mathbf{k}|)}\ . \tag{B7}$$

This expression for the linewidth $\Gamma(q)$ has a simple physical interpretation. The relaxation rate $\Gamma(q)$ of the fluctuations of wave vector $\mathbf{q}$ is given by the rate for it to de-

cay into fluctuations of wave vector $\mathbf{k}$ and $(\mathbf{q}-\mathbf{k})$, respectively. The vertex strength of this two-mode decay process is given by $v(k,q,\eta)$. Higher-order decay processes are neglected in this mode-coupling approach.

We are now in a position to obtain an expression of the energy scale function in the Lorentzian approximation, Ω_{Lor}. At $T=T_C$ we have, following Eqs. (4.11) and (4.13),

$$\chi(q)=\Upsilon q^{-2}$$

and (B8)

$$\hbar\Gamma(q)=\Omega_{\mathrm{Lor}}q^{5/2}\ .$$

Using these scaling relations in Eq. (B7), we derive

$$\Omega_{\mathrm{Lor}}^2=2\mathcal{J}a^2k_BT_C\frac{v}{4\pi^4}P^2 \tag{B9a}$$

with

$$P^2=2\pi^2\int_{-1}^{+1}d\eta\int_0^{\infty}\frac{dk}{q}v(q,k,\eta)\frac{q^2}{(\mathbf{q}-\mathbf{k})^2}\times\frac{q^{5/2}}{k^{5/2}+|\mathbf{q}-\mathbf{k}|^{5/2}}\ . \tag{B9b}$$

A numerical integration for P gives $P\cong 5.1326$. From Eq. (B9a) we obtain Eq. (4.14a).

*Present address: Institüt für Theoretische Physik, Physik-Department der Technischen Universität München, D-8046 Garching, Federal Republic of Germany.

[1]J. Kötzler, Phys. Rev. B **38**, 12 027 (1988), and references therein.
[2]C. Hohenemser, N. Rosov, and A. Kleinhammes, Hyperfine Interact. **49**, 267 (1989), and references therein.
[3]F. Mezei, J. Phys. (Paris) Colloq. **49**, C8-1537 (1988), and references therein.
[4]E. Frey and F. Schwabl, Phys. Lett. A **123**, 49 (1987); Z. Phys. B **71**, 355 (1988); **76**, 139E (1989); Hyperfine Interact. **50**, 767 (1989).
[5]E. Frey, F. Schwabl, and S. Thoma, Phys. Rev. B **40**, 7199 (1989).
[6]*Muon and Pions in Materials Research,* edited by J. Chappert and R. I. Grynszpan (North-Holland, Amsterdam, 1984).
[7]A. Schenck, *Muon Spin Rotation Spectroscopy* (Hilger, Bristol, 1985).
[8]K. Nishiyama, E. Yagi, K. Ishida, T. Matsuzaki, K. Nagamine, and T. Yamazaki, Hyperfine Interact. **17-19**, 473 (1984).
[9]D. Herlach, K. Fürderer, M. Fähnle, and L. Schimmele, Hyperfine Interact. **31**, 287 (1986).
[10]E. Wäckelgård, O. Hartmann, E. Karlsson, R. Wäppling, L. Asch, G. M. Kalvius, J. Chappert, and A. Yaouanc, Hyperfine Interact. **31**, 325 (1986).
[11]V. Yu. Yushankhai, Hyperfine Interact. **50**, 775 (1989).
[12]A. Yaouanc and P. Dalmas de Réotier, J. Phys.: Condens. Matter **3**, 6195 (1991).
[13]S. W. Lovesey, E. B. Karlsson, and K. N. Trohidou, J. Phys.: Condens. Matter **4**, 2043 (1992).
[14]S. W. Lovesey, K. N. Trohidou, and E. B. Karlsson, J. Phys.: Condens. Matter **4**, 2061 (1992).
[15]P. Dalmas de Réotier and A. Yaouanc, J. Phys.: Condens. Matter **4**, 4533 (1992).
[16]T. McMullen and E. Zaremba, Phys. Rev. B **18**, 3026 (1978).
[17]T. Moriya, Prog. Theor. Phys. (Kyoto) **28**, 371 (1962).
[18]M. Born and K. Huang, *Dynamical Theory of Crystal Lattices* (Clarendon, Oxford, 1954).
[19]A. Aharony and M. E. Fisher, Phys. Rev. B **8**, 3323 (1972).
[20]R. D. Misra, Proc. Cambridge Philos. Soc. **36**, 173 (1940).
[21]H. Kronmüller, H.-R. Hilzinger, P. Monachesi, and A. Seeger, Appl. Phys. **18**, 183 (1979).
[22]T. Holstein and H. Primakoff, Phys. Rev. **58**, 1098 (1940).
[23]M. H. Cohen and F. Keffer, Phys. Rev. **99**, 1128 (1955).
[24]L. M. Holmes, J. Als-Nielsen, and H. J. Guggenheim, Phys. Rev. B **12**, 180 (1975).
[25]See, for example, S. W. Lovesey, *Theory of Neutron Scattering from Condensed Matter* (Clarendon, Oxford, 1987), Vol. 1.
[26]P. Böni, D. Görlitz, J. Kötzler, and J. L. Martinez, Phys. Rev. B **43**, 8755 (1991).
[27]S. Thoma, E. Frey, and F. Schwabl, Phys. Rev. B **43**, 5831 (1991).
[28]J. Kötzler, D. Görlitz, F. Mezei, and B. Farago, Europhys. Lett. **1**, 675 (1986); **2**, 159E (1986).
[29]See, for example, S. W. Lovesey, *Condensed Matter Physics: Dynamic Correlations,* 2nd ed. (Benjamin/Cummings, New York, 1986).
[30]K. Kawasaki, in *Phase Transitions and Critical Phenomena,* edited by C. Domb and M. S. Green (Academic, New York, 1976), Vol. 5A.
[31]E. Frey and F. Schwabl (unpublished).
[32]D. Görlitz, J. Kötzler, F. J. Bermejo, P. Böni, and J. L. Martinez, Physica B **180&181**, 214 (1992).
[33]C. Kittel, *Introduction to Solid State Physics,* 4th ed. (Wiley, New York, 1971).
[34]L. Passell, O. W. Dietrich, and J. Als-Nielsen, Phys. Rev. B **14**, 4897 (1976), and references therein.
[35]F. Mezei, Physica B **136**, 417 (1986).
[36]J. P. Wicksted, P. Böni, and G. Shirane, Phys. Rev. B **30**, 3655 (1984).
[37]J. Als-Nielsen, in *Phase Transitions and Critical Phenomena,* edited by C. Domb and M. S. Green (Academic, New York, 1976), Vol. 5A.
[38]P. Böni, J. L. Martinez, and J. M. Tranquada, Phys. Rev. B **43**, 575 (1991).
[39]J. Als-Nielsen, O. W. Dietrich, and L. Passell, Phys. Rev. B **14**, 4908 (1976).
[40]A. B. Denison, H. Graf, W. Kündig, and P. F. Meier, Helv. Phys. Acta **52**, 460 (1979).
[41]F. Mezei, Phys. Rev. Lett. **49**, 1096 (1982).
[42]P. Böni and G. Shirane, Phys. Rev. B **33**, 3012 (1986).
[43]P. Böni, G. Shirane, H. G. Bohn, and W. Zinn, J. Appl. Phys. **61**, 3397 (1987).
[44]P. Böni, G. Shirane, H. G. Bohn, and W. Zinn, J. Appl. Phys. **63**, 3089 (1988).